



Science Arts & Métiers (SAM)

is an open access repository that collects the work of Arts et Métiers Institute of Technology researchers and makes it freely available over the web where possible.

This is an author-deposited version published in: <https://sam.ensam.eu>
Handle ID: <http://hdl.handle.net/10985/16656>

To cite this version :

Mohammad Saeid AGHIGHI, Amine AMMAR - Aspect ratio effects in Rayleigh-Bénard convection of Herschel-Bulkley fluids - Engineering Computations p.19 - 2017

Any correspondence concerning this service should be sent to the repository

Administrator : scienceouverte@ensam.eu



Aspect ratio effects in Rayleigh-Bénard convection of Herschel-Bulkley fluids

Mohammad Saeid Aghighi (Department of Mechanical Engineering, Bu Ali Sina University, Hamedan, Iran)
Amine Ammar (Arts et Métiers ParisTech, LAMPA, Angers, France)

Mohammad Saeid Aghighi, Amine Ammar, "Aspect ratio effects in Rayleigh-Bénard convection of Herschel-Bulkley fluids", Engineering Computations, <https://doi.org/10.1108/EC-06-2016-0227>

Aspect ratio effects in Rayleigh-Bénard convection of Herschel-Bulkley fluids

Abstract

Purpose – The purpose of this paper is to analyze two dimensional steady state Rayleigh-Bénard convection within rectangular enclosures in different aspect ratios filled with yield stress fluids obeying the Herschel-Bulkley model.

Design/methodology/approach – In this study, a numerical method based on the finite element has been developed for analyzing two dimensional natural convection of a Herschel-Bulkley fluid. The effects of Bingham number Bn and power law index n on heat and momentum transport have been investigated for a nominal Rayleigh number range ($5 * 10^3 < Ra < 10^5$) , three different aspect ratios (ratio of enclosure length:height $AR = 1, 2, 3$) and a single representative value of nominal Prandtl number ($Pr = 10$).

Findings – Results show that the mean Nusselt number \overline{Nu} increases with increasing Rayleigh number due to strengthening of convective transport. However, with the same nominal value of Ra the values of \overline{Nu} for shear thinning fluids $n < 1$ are greater than shear thickening fluids $n > 1$. The values of \overline{Nu} decrease with Bingham number and for large values of Bn , \overline{Nu} rapidly approaches to unity which is indicated that heat transfer takes place principally by thermal conduction. The effects of aspect ratios have also been investigated and results show that \overline{Nu} increases with increasing AR due to stronger convection effects.

Originality/value – Finite element analysis of viscoplastic fluids. Analysis of Rayleigh-Bernard flows involving Herschel-Bulkley fluids for a wide range of Rayleigh numbers, Bingham numbers and power law index. Study on the effects of aspect ratio on flow and heat transfer of Herschel-Bulkley fluids.

Keywords: Rayleigh-Bénard, Herschel-Bulkley, Aspect ratio, Finite element.

Paper type: Research paper.

1. Introduction

Viscoplastic fluids are characterized by a yield stress, the existence of a “yield stress” is traditionally recognized to be responsible for the complicated transition between classical solid-like and liquid-like behavior. If the material is not sufficiently stressed, it will not deform and behaves like a solid, but once the yield stress is exceeded, it will deform and flow according to different constitutive relations. Several systems and industrial processes are based on viscoplastic fluid behavior such as blood, drilling mud, mayonnaise, toothpaste, grease, and some lubricants. There are three ideal models based on viscoplastic model, the Bingham plastic, the Herschel- Bulkley model, and the Casson model (Mitsoulis 2007). Heat transfer analysis and especially convection had been one of the interesting parts of viscoplastic research works in last decades because of its applications, such as Nouar studies about combined forced and free convection heat transfer of a yield stress fluid (Nouar 2005) and thermal convection for an incompressible Herschel-Bulkley fluid along an annular duct (Nouar et al. 1998). In this field instability of necking processes for an elasto-viscoplastic lithosphere has been studied by Regenauer-Lieb and his co-worker (Regenauer-Lieb & Yuen 2000) and also, Soares et al. (Soares et al. 2003) have analyzed heat transfer in the entrance-region flow of Herschel-Bulkley fluids inside concentric annular spaces. Despite the number of researches carried out, information about natural convection process within a square enclosure containing viscoplastic material (especially for Herschel-Bulkley and Casson models) is still very scarce.

Rayleigh-Bénard convection as an important part of heat transfer has been investigated by some researchers. Actually Rayleigh-Bénard is a type of natural convection and occur in a fluid layer due to a horizontal temperature gradient, when the lower wall is heated and the upper wall cooled. First studies on this problem were motivated by the Bénard’s experiments around 1900 (Bénard 1900) who considered the stability of a fluid layer heated from below. A linear stability analysis was proposed in 1916 by Lord Rayleigh (Rayleigh 1916) underlying the buoyancy driven source of instability. The

first chapters of Chandrasekhar's book (Chandrasekhar 1961) present the linear theory within the Boussinesq approximation. Non-linear approaches were reviewed in (Busse 1978; Newell et al. 1993).

In the case of Newtonian and power law fluids, Aghighi et al. (Aghighi et al. 2013) solved transient and steady state Rayleigh-Bénard convection using the Proper Generalized Decomposition (PGD) method. They also analyzed the effects of nanoparticle's temperature and diameter on Rayleigh-Bénard convection of Nano-fluids (Aghighi et al. 2015). Before that, the RB convection along the isochore of nitrogen has been numerically studied by Shen and his co-worker (Shen & Zhang 2012) using the SIMPLE algorithm. The other numerical study has been done by Kao and Yang (Kao & Yang 2007). They used the lattice Boltzmann method to simulate the oscillatory flows of the secondary instability in 2D Rayleigh-Bénard convection. The steady state condition of two-dimensional Rayleigh-Bénard Convection was analyzed by Ouertatani et al. (Ouertatani et al. 2008) using finite volume method. There are also some experimental works such as Maystrenko et al. (Maystrenko et al. 2007) research about measurements of the temperature distribution in the upper (cold) boundary layer of a rectangular Rayleigh-Bénard cell for air in large aspect ratios.

While for Newtonian and Power law fluids we can refer several research studies, in the case of viscoplastic material there are no many research works especially for Herschel-Bulkley and Casson models. In the case of Bingham fluids the effects of a fluid yield stress on the classical Rayleigh-Bénard instability were examined by Zhang and his co-workers (Zhang et al. 2006) and Vikhansky (Vikhansky 2009) considered the effect of yield stress on the Rayleigh-Bénard convection of a viscoplastic material. A numerical analysis based on Fluent for Rayleigh-Bénard convection and Bingham model has been done by Turan et al. (Turan et al. 2012). Recently, the effects of aspect ratio on steady state Rayleigh-Bénard convection of Bingham fluids have been analyzed by Yigit et al. (Yigit et al. 2015) using Fluent simulation. Finally in the field of experimental study, Darbouli and his co-workers (Darbouli et al. 2013) have investigated the influence of rheological and interfacial properties of yield stress fluids on the onset of the Rayleigh-Bénard convection.

Besides developing a powerful numerical method based on the finite element which can be used

for analyzing different types of viscoplastic fluids, this study also investigated the effects of aspect ratio ($AR = 1, 2, 3$) on steady-state natural convection of yield stress fluids obeying the Herschel-Bulkley model within rectangular enclosures over wide ranges of conditions as: Rayleigh number, $5 * 10^3 < Ra < 10^5$, Bingham number, $0 < Bn < Bn_{max}$ and power law index, $0.7 < n < n_{max}$. To the best of our knowledge, it has not been studied before and the results reported here are new.

2. Mathematical formulation

The case under consideration is the two dimensional steady natural convection of a Herschel-Bulkley fluid, in a rectangular cavity (Figure 1). No-slip conditions are considered at walls. The cavity is heated from below and cooled from above. It is assumed that the viscous dissipation terms are negligible and fluid has constant properties (except the density changes which produce buoyancy forces).

Assuming the Boussinesq approximation and using the characteristic scales H for length, $u_0 = (g\beta H\Delta T)^{1/2}$ for the velocity, $t_0 = H/u_0$ for the time, and $p_0 = \rho u_0^2$ for the pressure, the dimensionless continuity, momentum and energy equations for Rayleigh-Bénard convection could be written as:

$$\begin{aligned}
 \frac{\partial u}{\partial x} + \frac{\partial v}{\partial y} &= 0 \\
 u \frac{\partial u}{\partial x} + v \frac{\partial u}{\partial y} &= -\frac{\partial p}{\partial x} + Pr^{\frac{n}{2}} Ra^{\frac{n-2}{2}} \left(\frac{\partial \tau_{xx}}{\partial x} + \frac{\partial \tau_{yx}}{\partial y} \right) \\
 u \frac{\partial v}{\partial x} + v \frac{\partial v}{\partial y} &= -\frac{\partial p}{\partial y} + Pr^{\frac{n}{2}} Ra^{\frac{n-2}{2}} \left(\frac{\partial \tau_{yy}}{\partial y} + \frac{\partial \tau_{xy}}{\partial x} \right) + \theta \\
 u \frac{\partial \theta}{\partial x} + v \frac{\partial \theta}{\partial y} &= (Ra.Pr)^{-1/2} \left(\frac{\partial^2 \theta}{\partial x^2} + \frac{\partial^2 \theta}{\partial y^2} \right)
 \end{aligned} \tag{1}$$

The steady state boundary conditions for this problem would be:

$u = v = 0$ at all walls

$$\frac{\partial \theta}{\partial x} = 0 \text{ at } x = 0 \text{ and } x = \frac{L}{H} = 1, 2, 3 \quad (2)$$

$$\theta = 0.5 \text{ at } y = 0$$

$$\theta = -0.5 \text{ at } y = 1$$

The Prandtl number, Pr , and Rayleigh number, Ra , defined by:

$$Pr = \frac{\mu C_p}{k} \quad (3)$$

$$Ra = \frac{g \beta \Delta T H^3}{\alpha \nu}$$

The various dimensional quantities above are defined as follows: u, v, θ and p are dimensionless horizontal velocity, vertical velocity, temperature and pressure respectively. μ is the dynamic viscosity, C_p is specific heat capacity, k is the thermal conductivity, g is the acceleration due to gravity, β is the coefficient of thermal expansion, α is the thermal diffusivity, ΔT is the temperature difference between hot and cool walls, ν is the kinematic viscosity, τ is the viscous stress and n is power law index.

The dimensionless temperature θ is defined by:

$$\theta = \frac{T - T_r}{T_H - T_C} \quad (4)$$

Where T_C and T_H ($T_H > T_C$) are the temperatures enforced at the top and bottom cavity boundaries, respectively, and T_r is a reference temperature: $T_r = (T_H + T_C)/2$.

The heat flux averaged over the hot wall is defined via the Nusselt number:

$$\overline{Nu} = - \int_0^1 \left. \frac{\partial \theta}{\partial y} \right|_{y=0} dx \quad (5)$$

The stress-deformation behavior of viscoplastic materials based on Herschel-Bulkley model is given by:

$$\tau_{ij} = \left(\dot{\gamma}^{n-1} + \frac{Bn}{\dot{\gamma}} \right) \dot{\gamma}_{ij} \quad \text{for} \quad |\tau| > \tau_y$$

(6)

and

$$\dot{\gamma} = 0 \quad \text{for} \quad |\tau| < \tau_y$$

For $i, j = 1, 2$ with $(x_1, x_2) = (x, y)$, where n is power law index, Bn Bingham number,

$$\dot{\gamma} = \sqrt{\frac{1}{2} \dot{\gamma}_{ij} \dot{\gamma}_{ij}} \quad \text{and} \quad \tau = \sqrt{\frac{1}{2} \tau_{ij} \tau_{ij}}.$$

The rate-of-strain tensor $\dot{\gamma}_{ij}$ is defined by:

$$\dot{\gamma}_{ij} = \frac{\partial u_i}{\partial x_j} + \frac{\partial u_j}{\partial x_i}$$

(7)

The dimensionless Bingham number Bn generally represents the ratio of yield stress to buoyancy stresses but based on equations (1) and (6) the value of $(Pr.Ra)^{-n/2}$ should be added to it so:

$$Bn = (Pr.Ra)^{-n/2} \frac{\tau_y}{\rho \beta g \Delta T H}$$

(8)

Papanastasiou modifications method (Papanastasiou 1987) can be applied to Herschel-Bulkley model to avoid discontinuity between yielded and unyielded regions. He proposed an exponential regularization of stress equation. based on this model equation (6) would be rewritten as:

$$\tau_{ij} = \left(\dot{\gamma}^{n-1} + \frac{Bn(1 - \exp(-m\dot{\gamma}))}{\dot{\gamma}} \right) \dot{\gamma}_{ij}$$

(9)

where m is regularization parameter and controls the exponential rise in the stress at low rates of strain.

While this model has been used by many researchers to analyze viscoplastic problems there are also other regularization techniques which circumvent the discontinuity inherent in these materials. The one which has gained wide acceptance in the literature is bi-viscous model. In this model, the unyielded material is assigned a very high value of viscosity. Comparison between the predictions of the yielded/unyielded regions using the two regularization techniques shows that the bi-viscous model is unable to identify the small unyielded regions as captured by the Papanastasiou regularization technique (Sairamu et al. 2013). However, these minor differences in the identification of yielded and

unyielded regions by the two techniques have very little influence on the value of the Nusselt number (Sairamu et al. 2013; Turan et al. 2012).

3. Numerical analysis

A numerical code based on the finite element method with quadrilateral, eight nodes elements was developed to solve the coupled conservation equations of mass, momentum and energy related to the two dimensional steady state Raleigh-Bénard convection within rectangular enclosures. When we proceed to the discretization of the weak form related to equation (1) some stability conditions must be ensured. One of them concerns the so-called LBB condition that restricts the free choice of pressure and velocity approximations. As in Aghighi et al. (Aghighi et al. 2013) in what follows we consider a penalty formulation of the incompressibility constraint. Thus, the equation (1) can be rewritten as below:

$$\begin{aligned}
\frac{\partial u}{\partial x} + \frac{\partial v}{\partial y} + \frac{1}{\lambda} p &= 0 \\
u \frac{\partial u}{\partial x} + v \frac{\partial u}{\partial y} + \frac{\partial p}{\partial x} &= Pr^{\frac{n}{2}} Ra^{\frac{n-2}{2}} \left(\frac{\partial \tau_{xx}}{\partial x} + \frac{\partial \tau_{yx}}{\partial y} \right) \\
u \frac{\partial v}{\partial x} + v \frac{\partial v}{\partial y} + \frac{\partial p}{\partial y} - \theta &= Pr^{\frac{n}{2}} Ra^{\frac{n-2}{2}} \left(\frac{\partial \tau_{yy}}{\partial y} + \frac{\partial \tau_{xy}}{\partial x} \right) \\
u \frac{\partial \theta}{\partial x} + v \frac{\partial \theta}{\partial y} - (Ra.Pr)^{-1/2} \left(\frac{\partial^2 \theta}{\partial x^2} + \frac{\partial^2 \theta}{\partial y^2} \right) &= 0
\end{aligned} \tag{10}$$

Where λ is a large enough constant. In this set of equations all variables are on the left side, but the stress terms on the right. The values of stress assumed to be known when the momentum equations analyzed. Initial values of velocity were considered to calculate shear rate and stress terms. Then, using the obtained values of stress and solving equations (10) the new values of velocity were computed. These new values were used to recompute stress terms and the process repeated until the values of velocity and temperature converge. It should be indicated that the numerical analysis of equations (10) in this format is not stable so the Laplace values of velocity were added to both sides of momentum equations these values does not affect the results but make the equation stable. The CPU

time shows that this convergence is very fast with an average of 400 second (Running on Mac 2.9 GHz Intel Core i5 and after about 1500 iteration). Using this method Rayleigh-Bénard convection has been analyzed successfully for viscoplastic fluids based on Herschel-Bulkley model in an enclosure with three different aspect ratios and results are presented below.

4. Results and discussion

4.1. Numerical method validation

Mesh convergence studies for each aspect ratio separately and based on the results, the meshes consist of 1825, 2133 and 2465 nodes have been used for $AR=1, 2, 3$ respectively.

The convergence of the solutions was checked by varying the penalty and regularization parameters. Results show that the \overline{Nu} value converges within 0.1% by varying λ from 10^3 to 10^4 and by varying m from 10^2 to 10^3 . In the following, all results are obtained for $\lambda = 10^4$ and $m = 10^3$.

To validate the numerical method Rayleigh-Bénard convection for Newtonian ($n = 1, Bn = 0, AR = 1$) and Bingham ($n = 1, AR = 1$) fluids was solved and the results compared with previous research works.

In the case of Newtonian fluids the results are compared with (Ouertatani et al. 2008) for several Rayleigh numbers and in all cases very good agreement can be determined. Results of Bingham fluids are compared with (Turan et al. 2012) where the Fluent base solution of Rayleigh-Bénard convection for Bingham fluids could be found. Results of non-dimensional velocity u , non-dimensional temperature θ and mean Nusselt number \overline{Nu} for $Ra = 5 * 10^4$ and $pr = 10$ are shown in figure 2 where the line shows the results of the present study and points show the Turan results.

4.2. Velocity and temperature

Due to the large number of results and to summarize, the results of velocity and temperature are only presented for mid-range Rayleigh number ($Ra = 5 * 10^4$).

One can see the effects of power law index in figure 3 where the variations of non-dimensional

velocity v and temperature θ along the horizontal and vertical mid-planes of the cavity are shown for different values of Power law index n at $AR = 1, 2, 3$ and $Bn = 0.5$. On the other hand, the effects of Bingham number are presented in figures 4 and 5 for shear thinning ($n = 0.85$) and shear thickening ($n = 1.05$) viscoplastic fluids respectively. It should be noted that while the power law index greater than one may not present real fluid behavior but the mathematical results are still considered to demonstrate the advantages of the present numerical method for solving the nonlinear complex models in critical conditions (critical power law index).

Comparing the results of figures 3-5 show that the magnitude of velocity increases with increasing AR due to stronger convection force there are also more maximum (and minimum) points of velocity because of more convection rolls in the enclosure where the numbers of convection rolls are equal to the value of aspect ratio. It should be noted that the vertical mid-plane of the enclosure passes through the center of convection roll when $AR = 1$ and 3 , but from the boundary of them when $AR = 2$ so different distribution of the temperature can be seen.

One can see that the magnitude of velocity and non-linearity of temperature distribution decrease with increasing power law index (or Bingham number) indicating weakening of convective thermal transport due to the additional flow resistance and this trend strengthens with increasing power law index (Bingham number) cause flow tend toward the rest condition and temperature towards the linear variation with x/L which is indicated that the relative contribution of thermal conduction to the overall heat transfer increases with increasing power law index (Bingham number).

For high value of power law index (Bingham number), the viscous forces overcome the buoyancy force and as a result of this, the heat transfer is due to thermal conduction and there is no significant flow within the enclosure. One can find this result from figures 3-5 where the temperature distribution becomes linear and the magnitude of velocity converge to zero. For linear distribution of temperature, the mean Nusselt number approach to unity which means that the heat transfer is due to thermal conduction. The value of power law index or Bingham number at which \overline{Nu} approaches to $\overline{Nu} = 1$ is defined as critical power law index (n_{max}) or critical Bingham number (Bn_{max}). Comparing the

results from figures 3-5 show that the value of n_{max} or Bn_{max} increases with increasing AR due to the stronger convection force which can overcome the flow resistance up to greater values of power law index (Bingham number). More details about heat transfer and mean Nusselt number are presented in the next section.

4.3. Heat transfer (Nusselt number)

The results are presented in two parts. First, the effects of power-law index n are shown for three selected Bingham numbers (non-yielded fluids, middle range and close to the critical Bingham number). Then the effects of Bingham number Bn are presented for three power law index: $n = 0.85$ (middle range of shear thinning fluids $n < 1$), $n = 1$ (Bingham fluids) and $n = 1.05$ (close to the critical power law index for $Bn > 0$).

The variation of mean Nusselt number \overline{Nu} with Power law index n is shown in figure 6 for $Ra = 5 * 10^3$ (with selected Bingham numbers: $Bn = 0, 0.04, 0.08$) and for $Ra = 10^4$ (with selected Bingham numbers: $Bn = 0, 0.1, 0.2$). Same results are presented in figure 7 for $Ra = 5 * 10^4$ ($Bn = 0, 0.5, 1.0$) and $Ra = 10^5$ ($Bn = 0, 0.75, 1.5$). It can be seen that the maximum of the mean Nusselt number occurs in shear thinning fluids where $n = 0.7$. The mean Nusselt number decreases with increasing power law index which indicates that convective thermal transport has been weak due to augmented viscous resistance. While for non-yielded power law fluids ($Bn = 0$) the value of mean Nusselt number decreases gradually (and so it is limited to the amount proportional to $n = 1.18$) for viscoplastic fluids, the value of mean Nusselt number rapidly approaches unity $\overline{Nu} = 1$ when power law index increases as thermal conduction becomes the dominant mode of heat transfer.

The variation of mean Nusselt number \overline{Nu} with Bingham number Bn is shown in figure 8 for different values of power law index ($n = 0.85, 1, 1.05$) and aspect ratio ($AR = 1, 2, 3$) at $Ra = 5 * 10^3, 10^4$ and same results are presented in figure 9 for $Ra = 5 * 10^4, 10^5$. It can be seen that the maximum of the mean Nusselt number occurs in non-yielded fluids where $Bn = 0$ and for viscoplastic fluids $Bn > 0$ the mean Nusselt number decreases with increasing Bingham number.

Comparing the results of figures 6-9 show that for a given set of values of Ra, n and Bn , the value of mean Nusselt number increases with increasing aspect ratio because the strength of the convection rolls increase with increasing AR , which can improve the quality of the heat transfer within the enclosure, as a result of this, there is an extended range of power law index (Bingham number) for convective transport in the cavity before dropping to $\overline{Nu} = 1$. Results of different Rayleigh numbers show that the mean Nusselt number increases with increasing Ra because of stronger buoyancy effects which can surpass the yield stress effects. It can also be seen that for shear thinning fluids ($n < 1$) the effects of Bingham number on heat transfer decrease with decreasing Rayleigh number.

Results show that the mean Nusselt number decreases with increasing power law index (Bingham number) and for large value of power law index $n \geq n_{max}$ (Bingham number $Bn \geq Bn_{max}$) the value of mean Nusselt number rapidly approaches unity $\overline{Nu} = 1$ as thermal conduction becomes the dominant mode of heat transfer. Comparing the results of different Rayleigh numbers and aspect ratios show that the values of n_{max} and Bn_{max} increase with increasing Ra and AR .

5. Contours of temperature and velocity vectors

Figures 10 and 11 show contours of non-dimensional temperature θ and velocity vectors for three different values of aspect ratio ($AR = 1, 2, 3$) and power law index ($n = 0.85, 1, 1.05$) at $Ra = 5 * 10^4$ and $Bn = 0.25$. The black lines in these figures show the plug regions (TUR and AUR) where $\tau < \tau_y$. The truly unyielded regions (TUR) move with a plug velocity profile (no deformation), and the apparently unyielded regions (AUR) are in the corners, where the velocities are very small, so the area behaves as stagnant, and no deformation occurs (Mitsoulis 2007). One can see that the isothermal lines become more curved and plug regions decrease with decreasing n because of the low viscosity effects. Furthermore, the number of convection rolls within the enclosure change with AR and thus the qualitative nature of isothermal line and velocity vectors have also changed with AR . It can be observed that increase in AR generally decrease plug regions due to stronger convection effects.

6. Conclusions

In this study a finite element numerical code has been developed for analyzing two dimensional steady state natural convection of viscoplastic fluids obeying the Herschel-Bulkley model within rectangular enclosures heated from below and cooled from above at constant temperature.

The effects of Bingham number Bn , power law index n and aspect ratio AR (length: height) on heat and momentum transport have been investigated in the nominal Rayleigh number range ($5 * 10^3 < Ra < 10^5$) for a single representative value of nominal Prandtl number ($Pr = 10$). Results show that the mean Nusselt number \overline{Nu} increases with increasing Rayleigh number due to stronger convection effects and decreases with increasing power law index because of strengthening viscous forces. For a given set of values of the Rayleigh number Ra and power law index n the mean Nusselt number \overline{Nu} is found to decrease with increasing values of the Bingham number. Results show that for a large value of power law index ($n \geq n_{max}$) or Bingham number ($Bn \geq Bn_{max}$) the value of mean Nusselt number rapidly approaches unity ($\overline{Nu} = 1$) which means that the dominant mode of heat transfer in the enclosure is thermal conduction. The values of n_{max} and Bn_{max} depends on Ra , and increase with increasing Ra due to stronger convection effects. The effects of aspect ratio on momentum and thermal transport have also been investigated in detail. The number of convection rolls and mean Nusselt numbers are found to increase with increasing AR for a given set of values of Ra and power law index n . Results also show that for shear thinning fluids ($n < 1$) the effects of Bingham number on heat transfer decrease with decreasing Rayleigh number.

References

- Aghighi, M.S. et al., 2013. Non-incremental transient solution of the Rayleigh–Bénard convection model by using the PGD. *Journal of Non-Newtonian Fluid Mechanics*, 200, pp.65–78.
- Aghighi, M.S. et al., 2015. Parametric solution of the Rayleigh-Benard convection model by using the PGD Application to nanofluids. *International Journal of Numerical Methods for Heat & Fluid Flow*, 25(6), pp.1252–1281.

- Bénard, H., 1900. Les tourbillons cellulaires dans une nappe liquide. *Rev. Gén. Sci. pures et appl.*, 11, pp.1261–1271, 1309–1328.
- Busse, F.H., 1978. Non-linear properties of thermal convection. *Reports on Progress in Physics*, 41(12), pp.1929–1967.
- Chandrasekhar, S., 1961. *Hydrodynamic and Hydromagnetic Stability*, Oxford: Clarendon.
- Darbouli, M. et al., 2013. Rayleigh-Bénard convection for viscoplastic fluids. *Physics of Fluids*, 25(2), p.23101.
- Kao, P.-H. & Yang, R.-J., 2007. Simulating oscillatory flows in Rayleigh-Bénard convection using the lattice Boltzmann method. *International Journal of Heat and Mass Transfer*, 50(17–18), pp.3315–3328.
- Maystrenko, A., Resagk, C. & Thess, A., 2007. Structure of the thermal boundary layer for turbulent Rayleigh-Bénard convection of air in a long rectangular enclosure. *Physical Review E*, 75(6), p.66303.
- Mitsoulis, E., 2007. Flows of viscoplastic materials: models and computations. *The British Society of Rheology*, 2007, pp.135–178.
- Newell, A.C., Passot, T. & Lega, J., 1993. Order Parameter Equations for Patterns. *Annual Review of Fluid Mechanics*, 25(1), pp.399–453.
- Nouar, C., 2005. Thermal convection for a thermo-dependent yield stress fluid in an axisymmetric horizontal duct. *International Journal of Heat and Mass Transfer*, 48(25–26), pp.5520–5535.
- Nouar, C., Desaubry, C. & Zenaidi, H., 1998. Numerical and experimental investigation of thermal convection for a thermodependent Herschel-Bulkley fluid in an annular duct with rotating inner cylinder. *European Journal of Mechanics - B/Fluids*, 17(6), pp.875–900.
- Ouertatani, N. et al., 2008. Numerical simulation of two-dimensional Rayleigh-Bénard convection in an enclosure. *Comptes Rendus Mécanique*, 336(5), pp.464–470.
- Papanastasiou, T.C., 1987. Flows of Materials with Yield. *Journal of Rheology*, 31(5), p.385.
- Rayleigh, Lord, 1916. On the convective currents in a horizontal layer of fluid when the higher

temperature is on the underside. *Phil. Mag.*, 32, pp.529–546.

Regenauer-Lieb, K. & Yuen, D. a., 2000. Quasi-adiabatic instabilities associated with necking processes of an elasto-viscoplastic lithosphere. *Physics of the Earth and Planetary Interiors*, 118(1–2), pp.89–102.

Sairamu, M., Nirmalkar, N. & Chhabra, R.P., 2013. Natural convection from a circular cylinder in confined Bingham plastic fluids. *International Journal of Heat and Mass Transfer*.

Shen, B. & Zhang, P., 2012. Rayleigh–Bénard convection in a supercritical fluid along its critical isochore in a shallow cavity. *International Journal of Heat and Mass Transfer*, 55(23–24), pp.7151–7165.

Soares, E.J., Naccache, M.F. & Souza Mendes, P.R., 2003. Heat transfer to viscoplastic materials flowing axially through concentric annuli. *International Journal of Heat and Fluid Flow*, 24(5), pp.762–773.

Turan, O., Chakraborty, N. & Poole, R.J., 2012. Laminar Rayleigh–Bénard convection of yield stress fluids in a square enclosure. *Journal of Non-Newtonian Fluid Mechanics*, 171–172, pp.83–96.

Vikhansky, a., 2009. Thermal convection of a viscoplastic liquid with high Rayleigh and Bingham numbers. *Physics of Fluids*, 21(10), p.103103.

Yigit, S., Poole, R.J. & Chakraborty, N., 2015. Effects of aspect ratio on natural convection of Bingham fluids in rectangular enclosures with differentially heated horizontal walls heated from below. *International Journal of Heat and Mass Transfer*, 80, pp.727–736.

Zhang, J., Vola, D. & Frigaard, I. a., 2006. Yield stress effects on Rayleigh–Bénard convection. *Journal of Fluid Mechanics*, 566, pp.389–419.

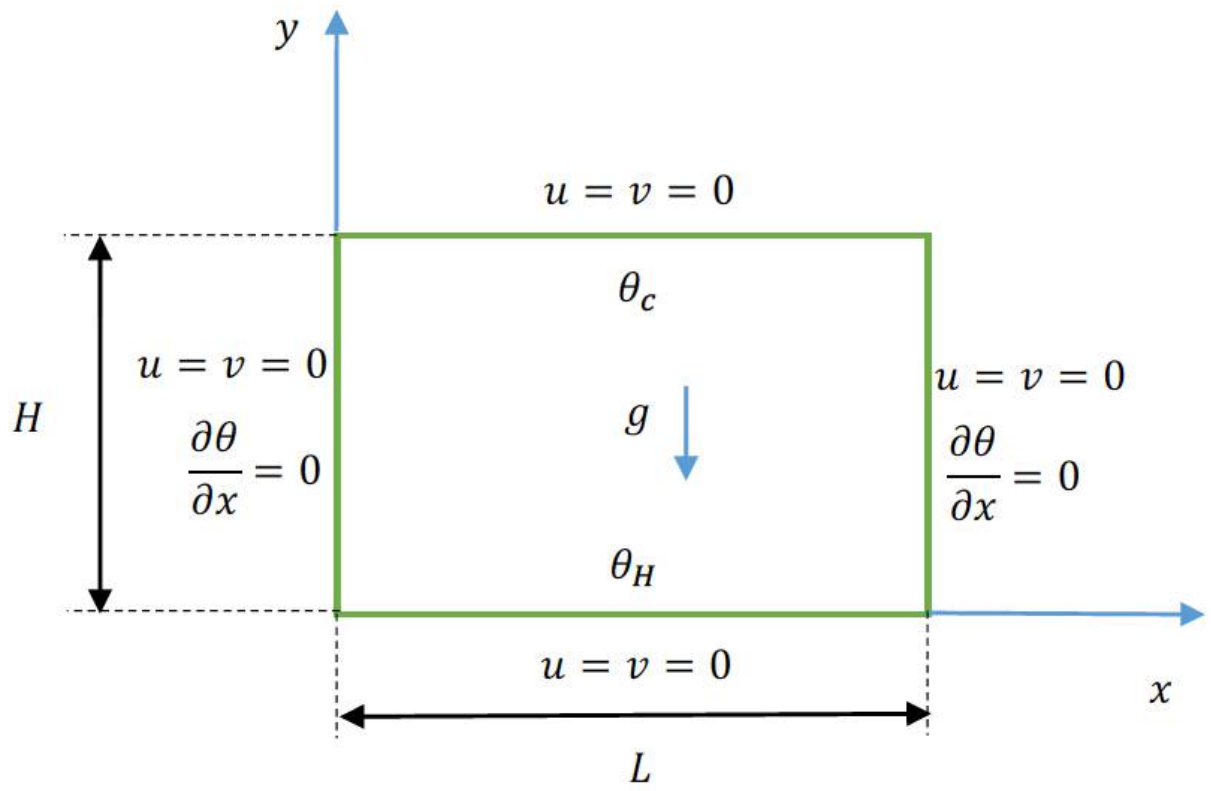


Figure 1: Schematic diagram of the physical model and coordinate system.

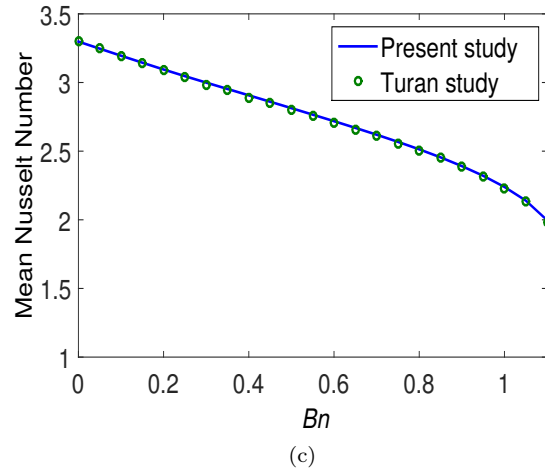
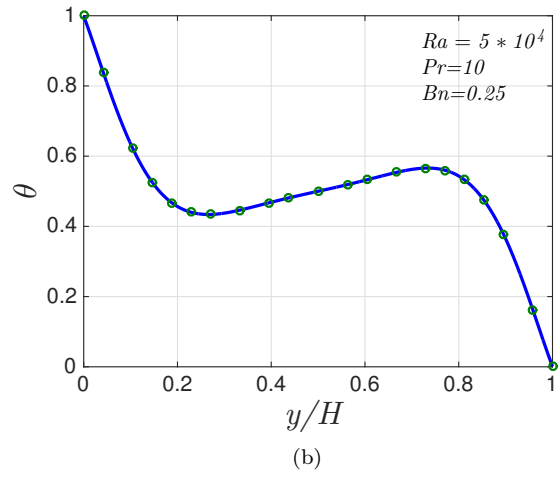
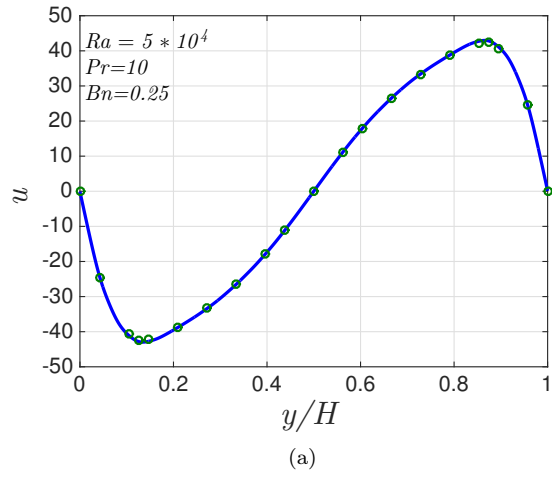
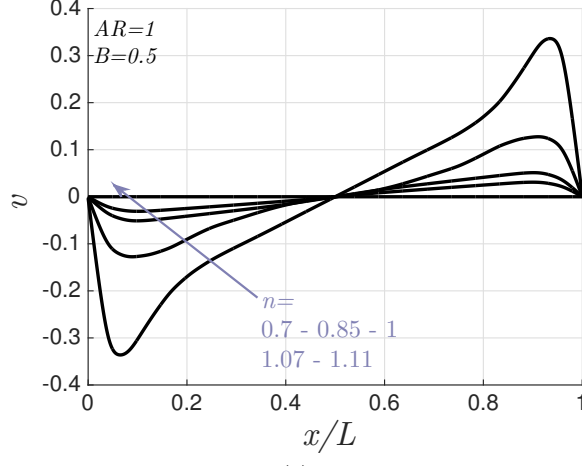
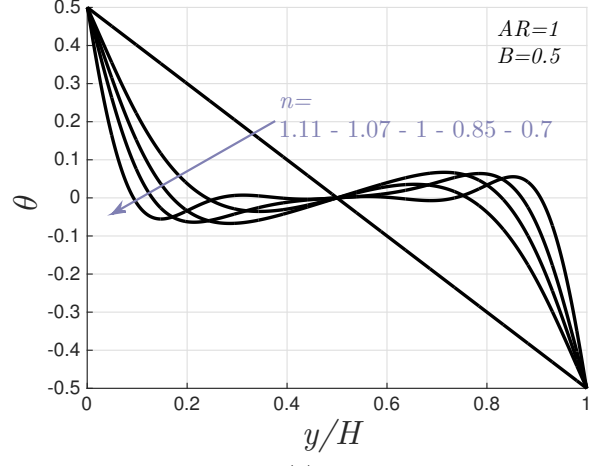


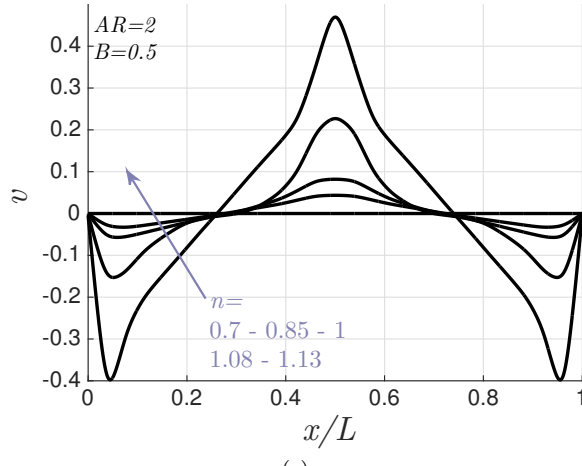
Figure 2: Variations of non-dimensional velocity u , non-dimensional temperature θ and mean Nusselt number \overline{Nu} for Bingham fluids at $Ra = 5 * 10^4$ and $pr = 10$ (line: present study, points: Turan study).



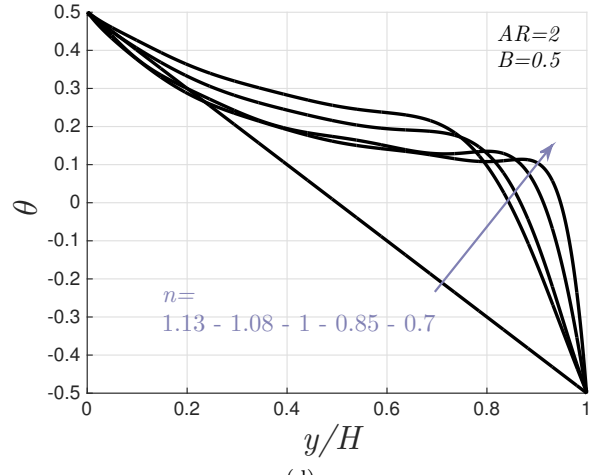
(a)



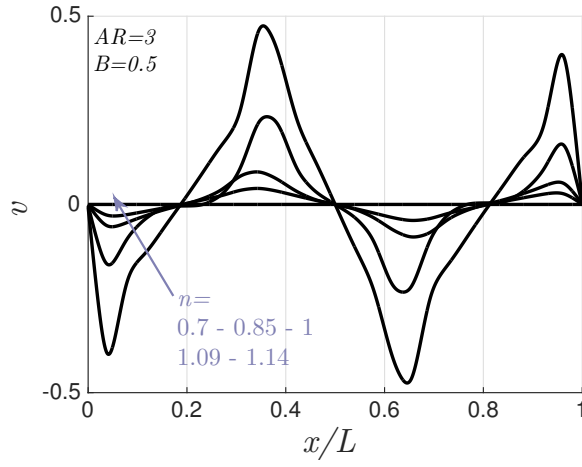
(b)



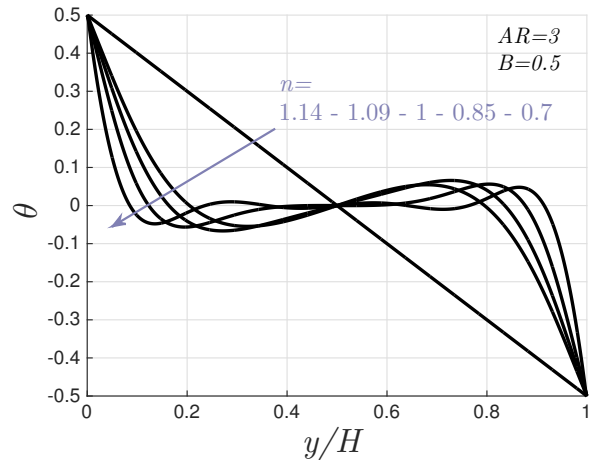
(c)



(d)

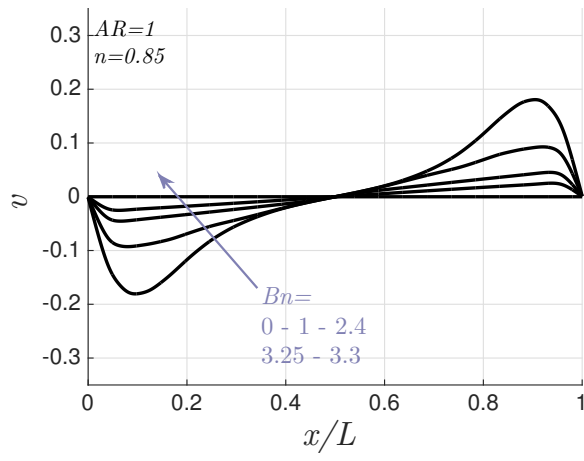


(e)

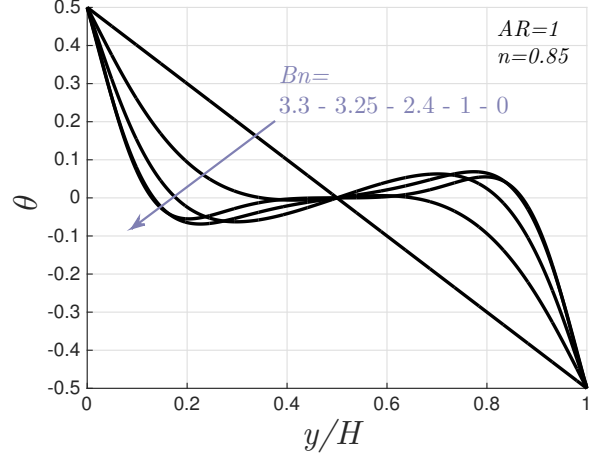


(f)

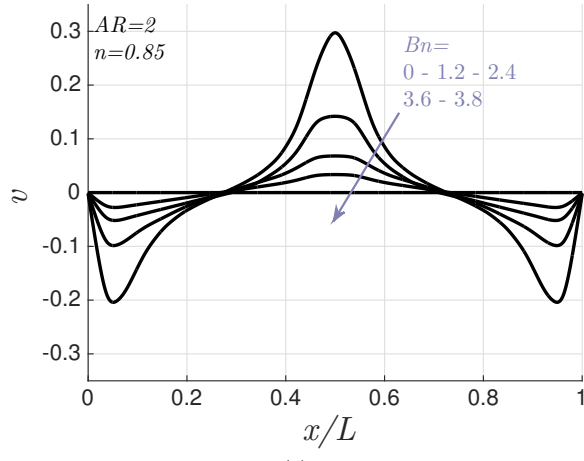
Figure 3: Variations of non-dimensional velocity v and temperature θ with power law index n along the horizontal and vertical mid-planes for three different values of aspect ratio ($AR = 1, 2, 3$) at $Ra = 5 \times 10^4$ and $Bn = 0.5$.



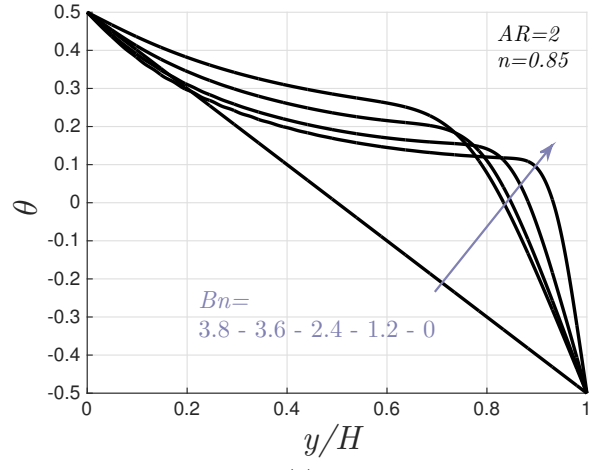
(a)



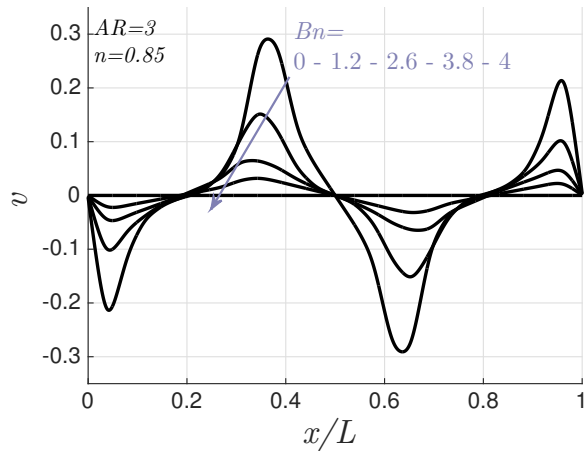
(b)



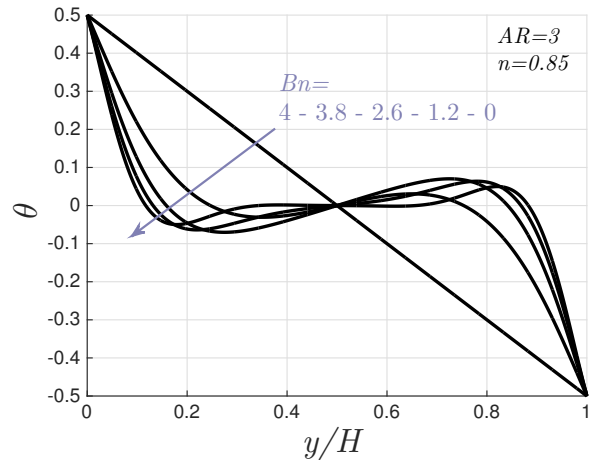
(c)



(d)

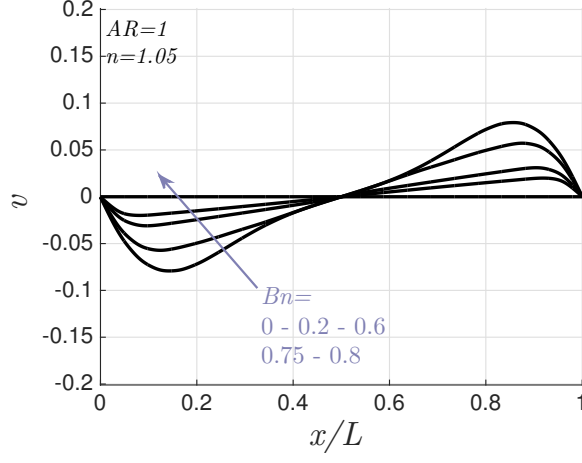


(e)

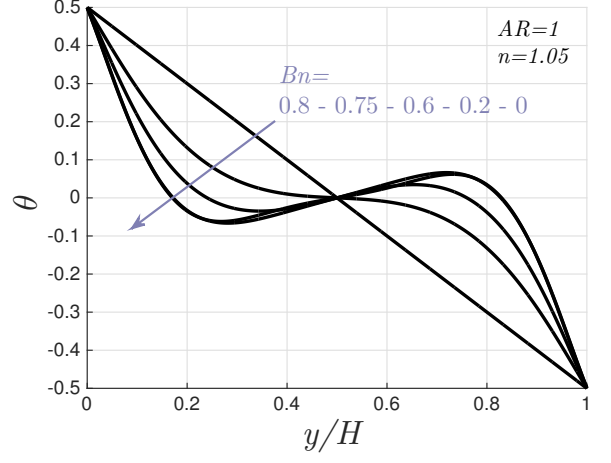


(f)

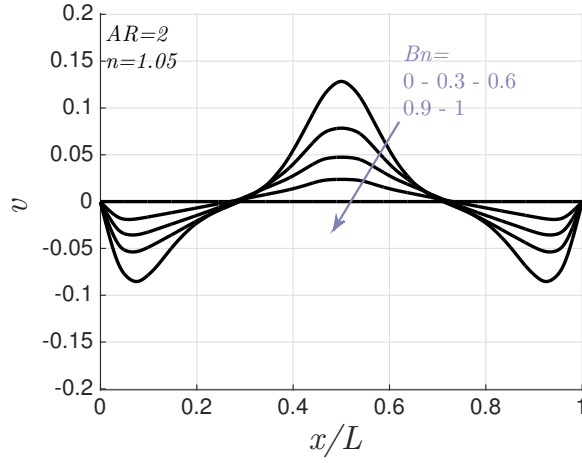
Figure 4: Variations of non-dimensional velocity v and temperature θ with Bingham number Bn along the horizontal and vertical mid-planes for three different values of aspect ratio ($AR = 1, 2, 3$) at $Ra = 5 \times 10^4$ and $n = 0.85$.



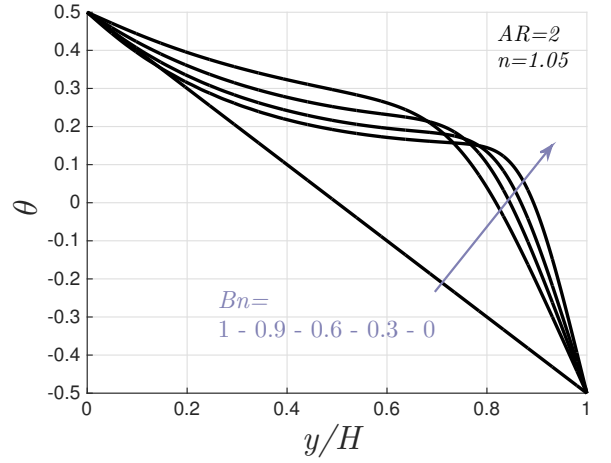
(a)



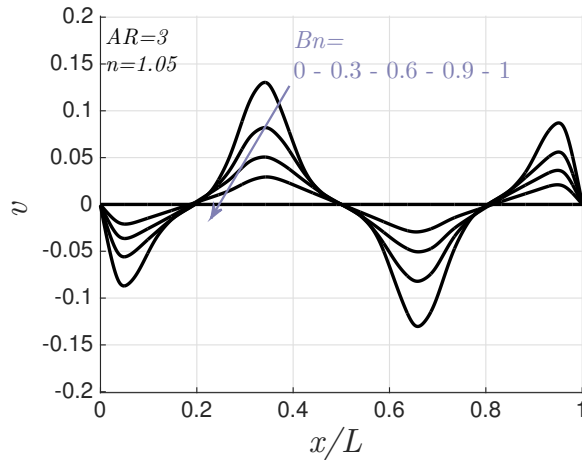
(b)



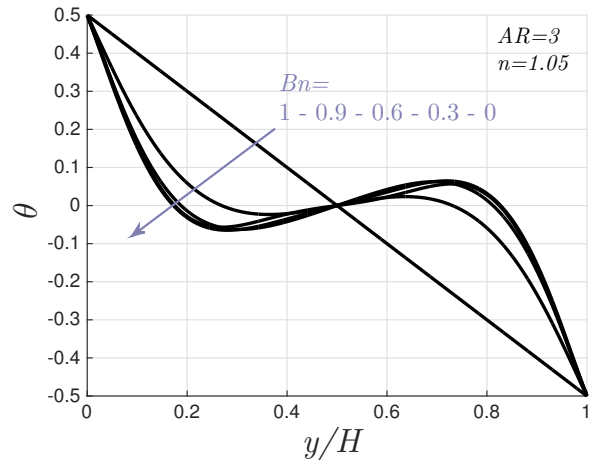
(c)



(d)

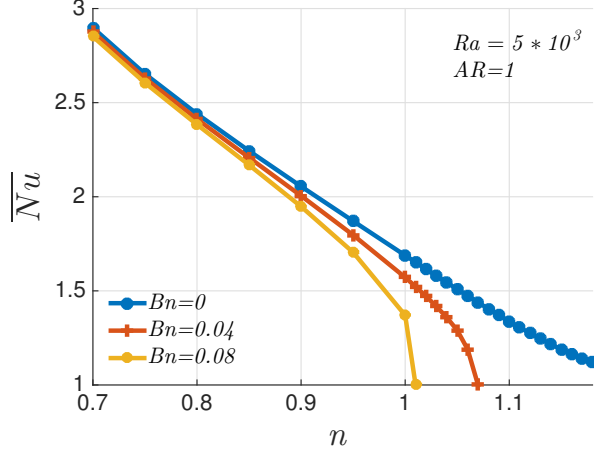


(e)

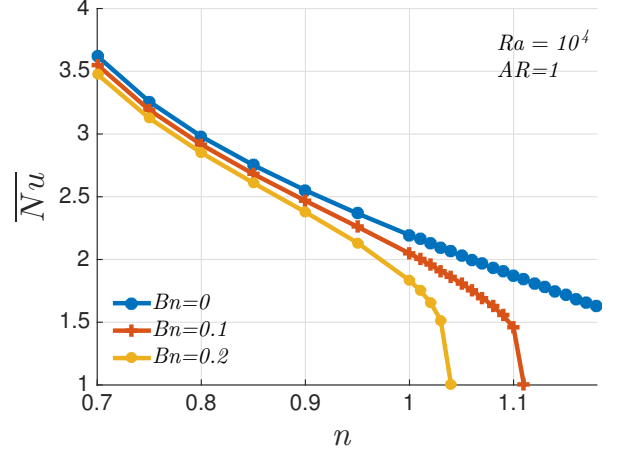


(f)

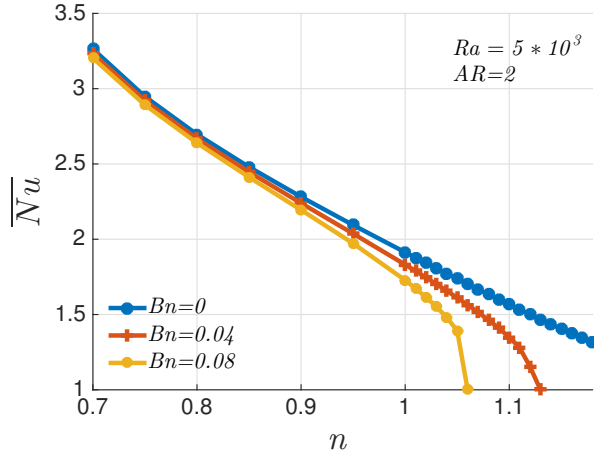
Figure 5: Variations of non-dimensional velocity v and temperature θ with Bingham number Bn along the horizontal and vertical mid-planes for three different values of aspect ratio ($AR = 1, 2, 3$) at $Ra = 5 \times 10^4$ and $n = 1.05$.



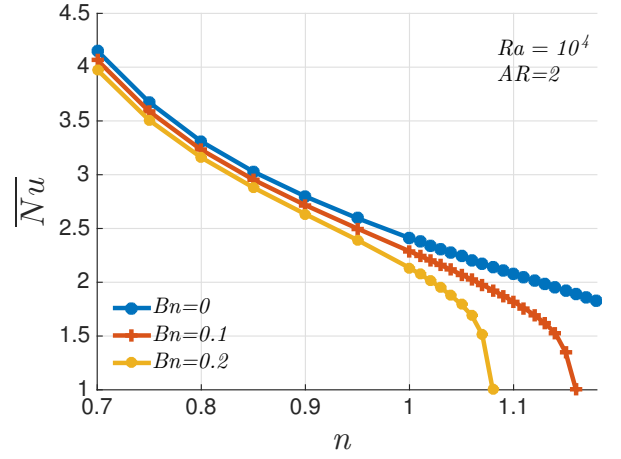
(a)



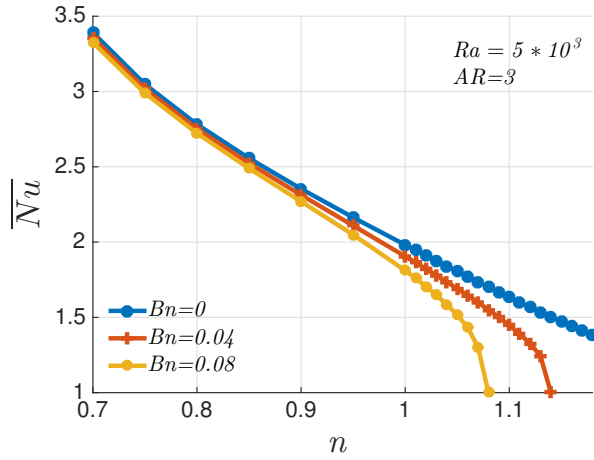
(b)



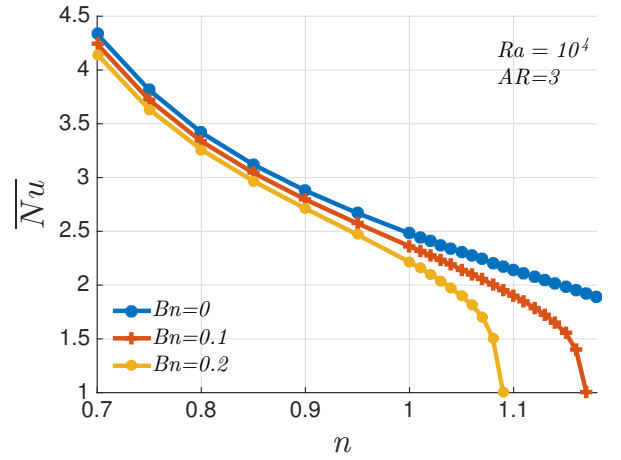
(c)



(d)

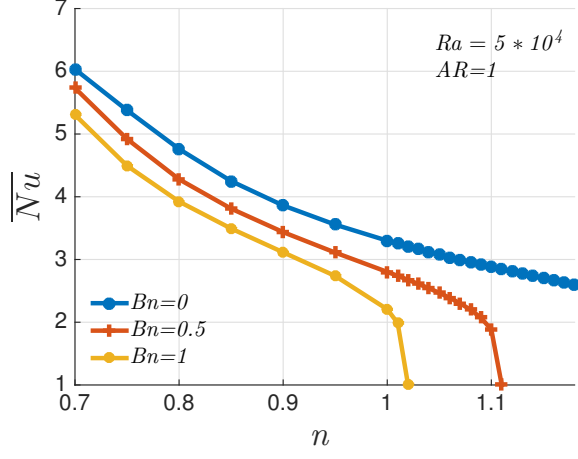


(e)

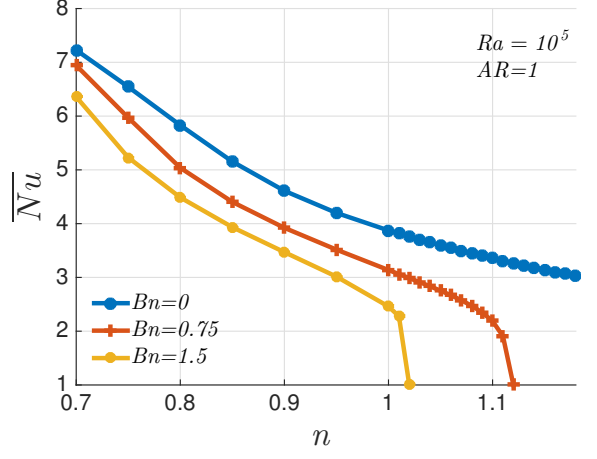


(f)

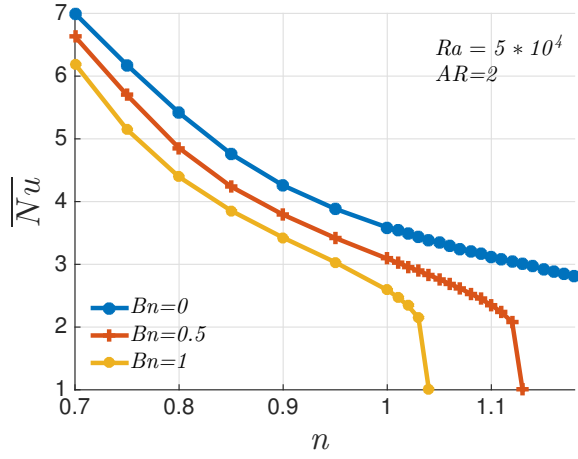
Figure 6: Evolution of the mean Nusselt number with the power law index for three different values of aspect ratio and Bingham number at $Ra = 5 * 10^3$ (left) and $Ra = 10^4$ (right).



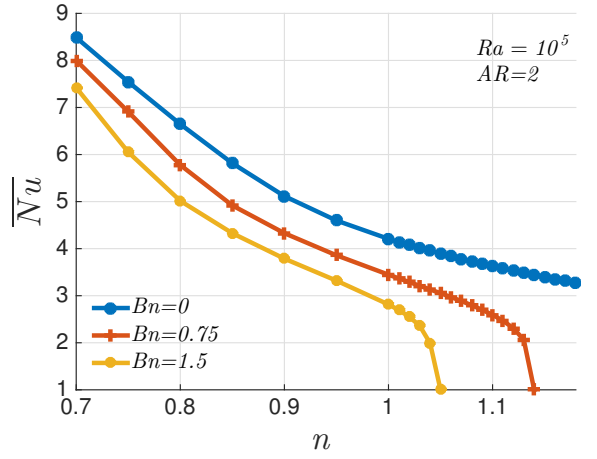
(a)



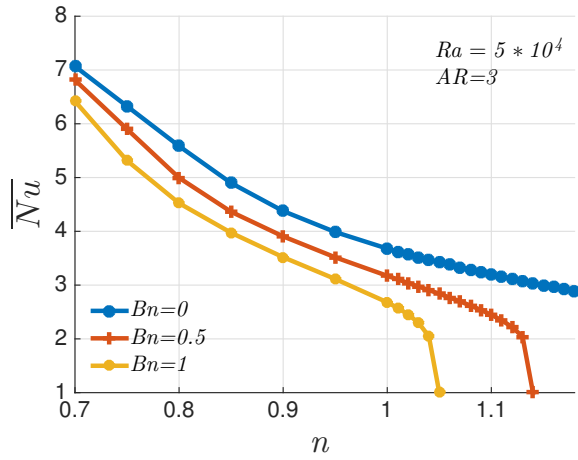
(b)



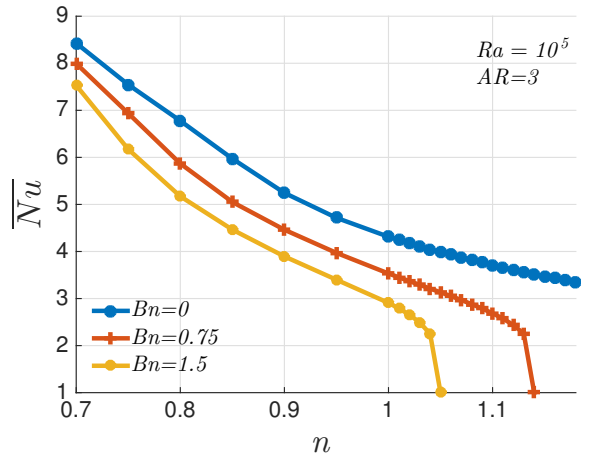
(c)



(d)



(e)



(f)

Figure 7: Evolution of the mean Nusselt number with the power law index for three different values of aspect ratio and Bingham number at $Ra = 5 * 10^4$ (left) and $Ra = 10^5$ (right).

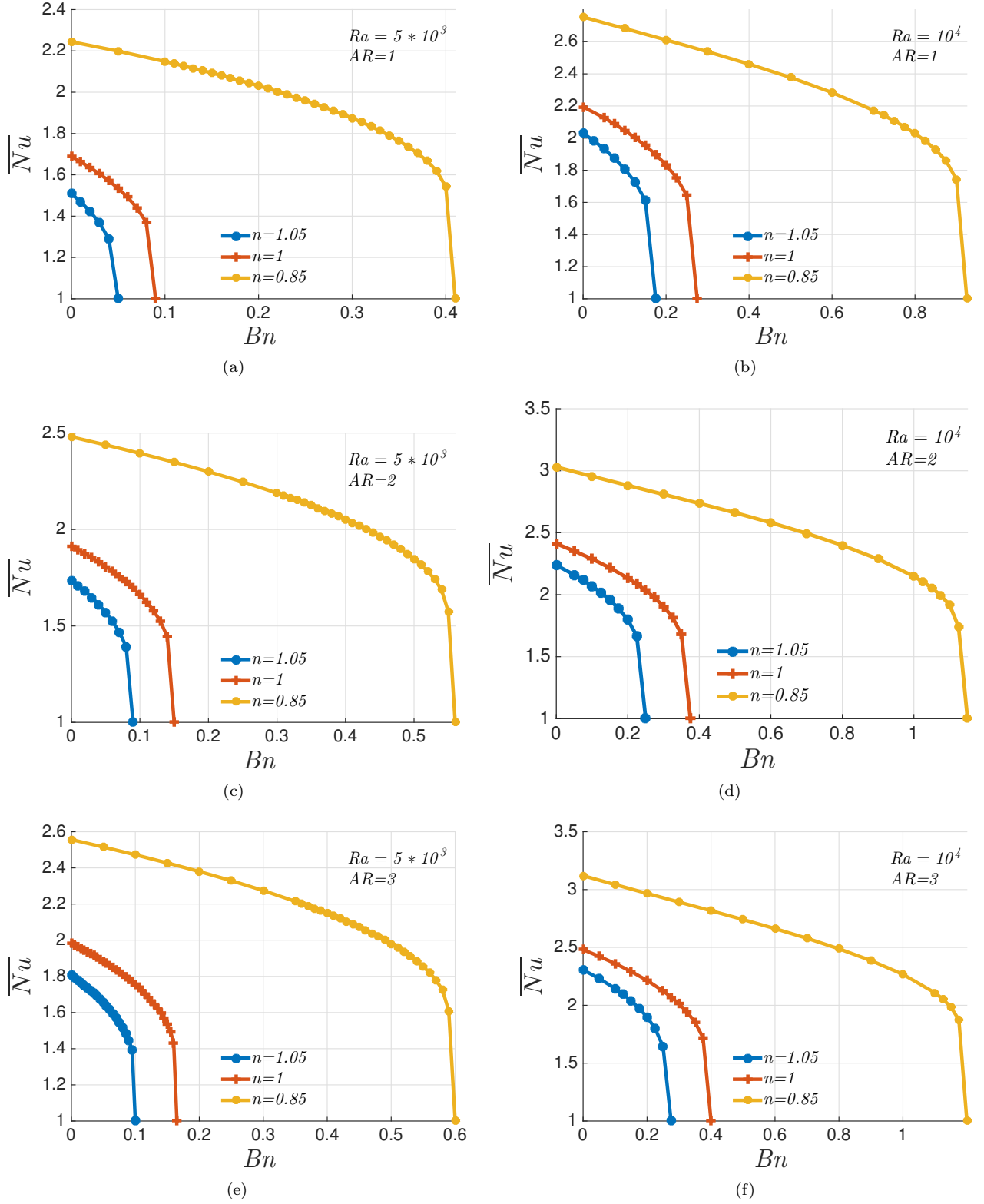
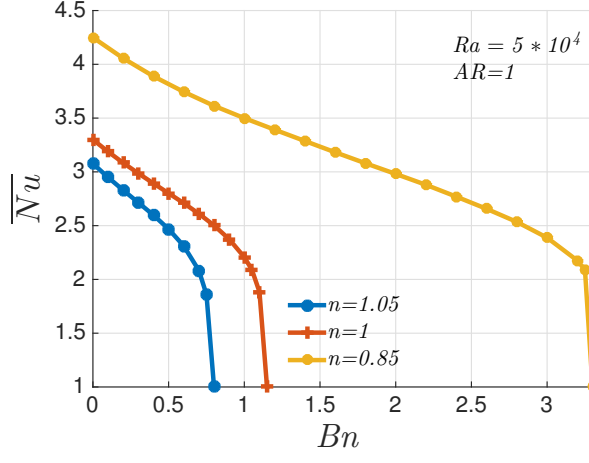
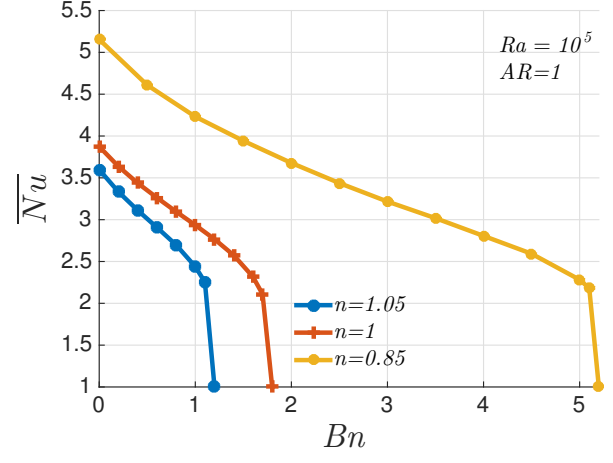


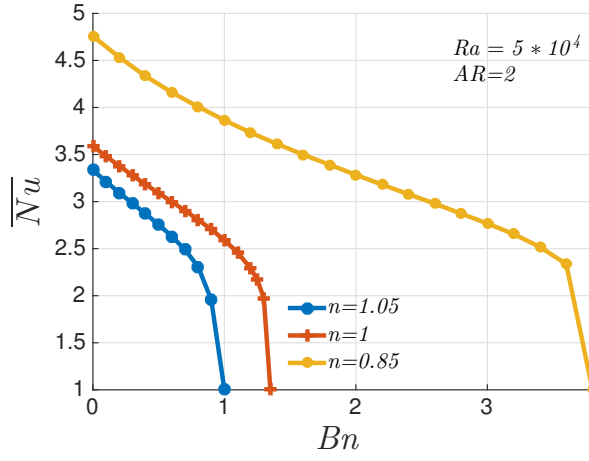
Figure 8: Evolution of the mean Nusselt number with the Bingham number for three different values of aspect ratio and power law index at $Ra = 5 * 10^3$ (left) and $Ra = 10^4$ (right).



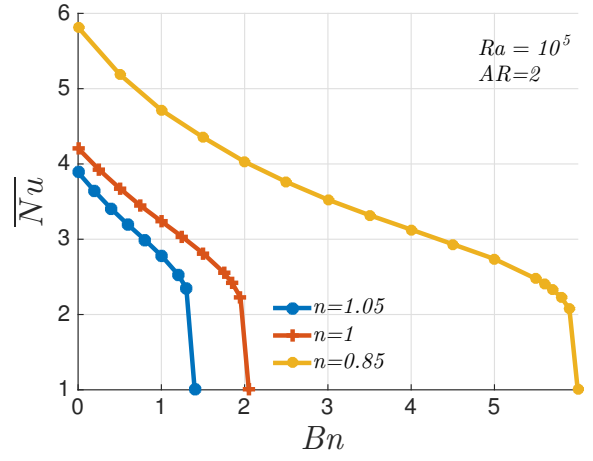
(a)



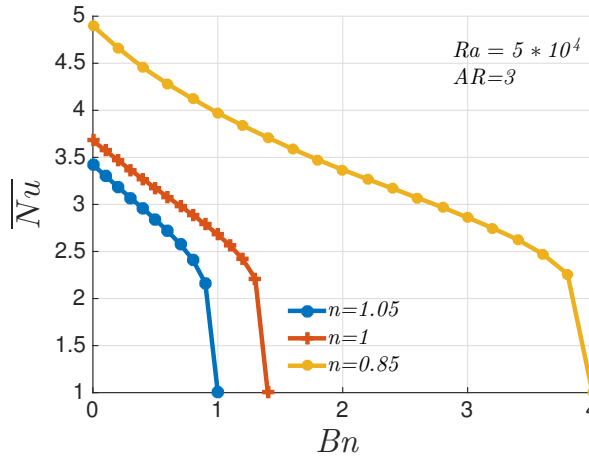
(b)



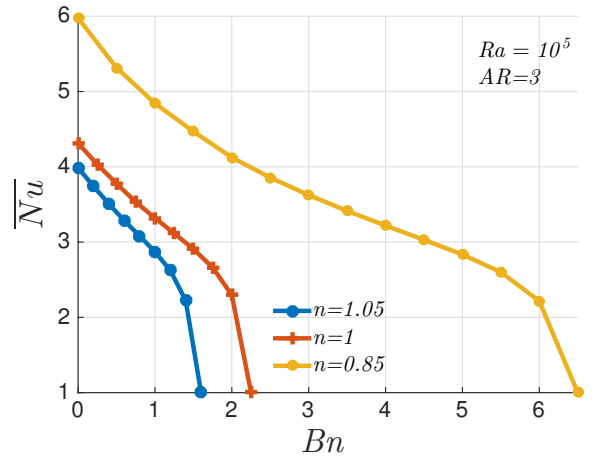
(c)



(d)

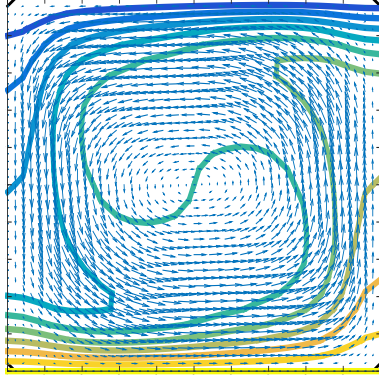


(e)

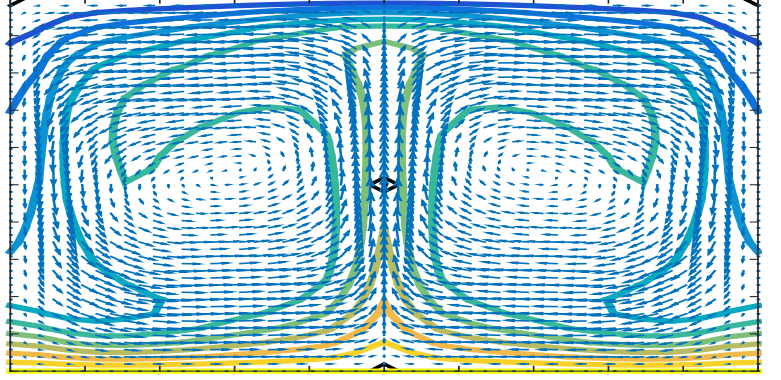


(f)

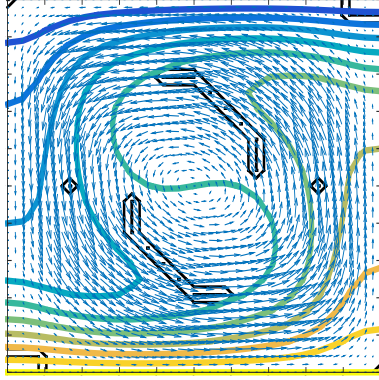
Figure 9: Evolution of the mean Nusselt number with the Bingham number for three different values of aspect ratio and power law index at $Ra = 5 * 10^4$ (left) and $Ra = 10^5$ (right).



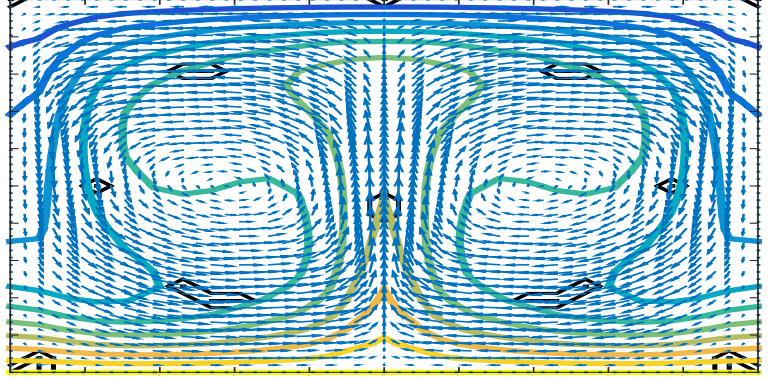
(a) $AR = 1, n = 0.85$



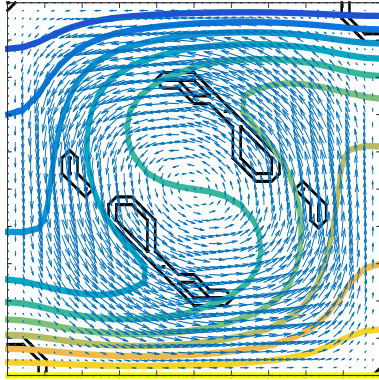
(b) $AR = 2, n = 0.85$



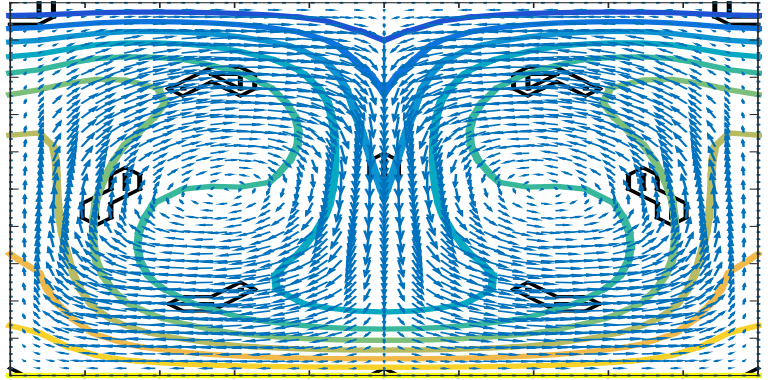
(c) $AR = 1, n = 1$



(d) $AR = 2, n = 1$

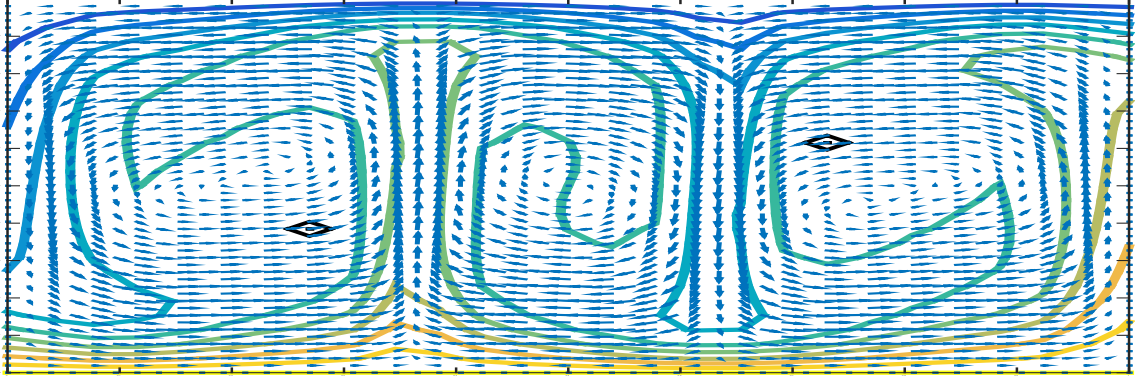


(e) $AR = 1, n = 1.05$

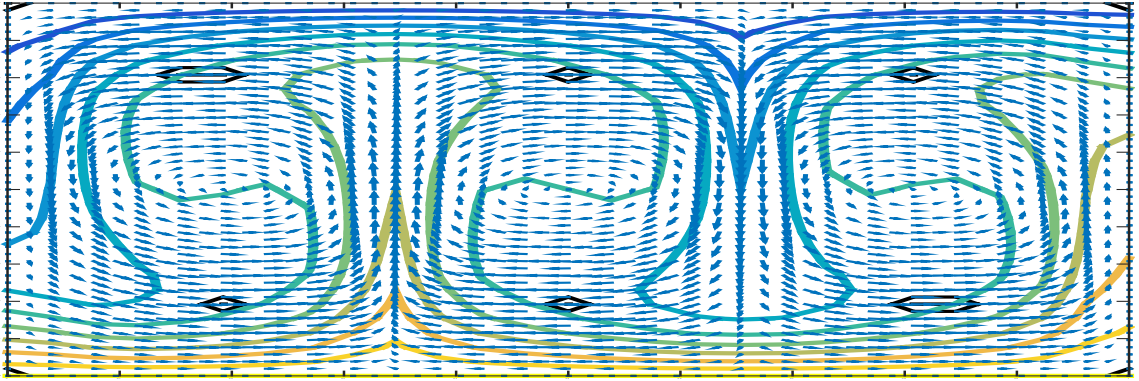


(f) $AR = 2, n = 1.05$

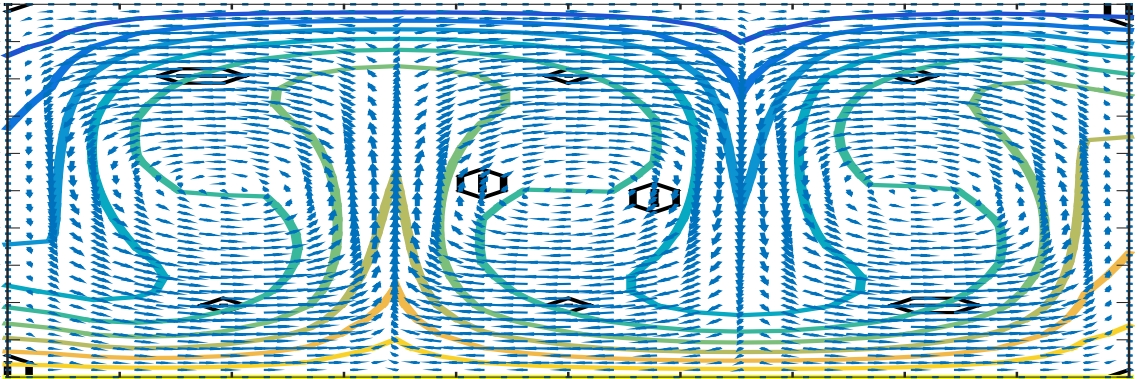
Figure 10: Contours of non-dimensional temperature θ and velocity vectors with plug regions (shown with black lines) for $AR = 1$ (on the left) and $AR = 2$ (on the right) and three different values of power law index ($n = 0.85, 1, 1.05$) at $Bn = 0.25$ and $Ra = 5 \times 10^4$.



(a) $AR = 3, n = 0.85$



(b) $AR = 3, n = 1$



(c) $AR = 3, n = 1.05$

Figure 11: Contours of non-dimensional temperature θ and velocity vectors with plug regions (shown with black lines) for $AR = 3$ and three different values of power law index ($n = 0.85, 1, 1.05$) at $Bn = 0.25$ and $Ra = 5 * 10^4$.